Journal of NAMP 67, 2 (2024) 199-206

The Nigerian Association of Mathematical Physics

Journal homepage: https://nampjournals.org.ng

Development of Detection Model for emphysema patterns in Computed Tomography Images

Musibau A. Ibrahim*[1], Oladotun A. Ojo[2], Peter A. Oluwafisoye[2]

[1]*Department of Computer Science, Osun State University, Osogbo, Nigeria*

[2]*Department of Physics, Osun State University, Osogbo, Nigeria.*

ARTICLE INFO

Article history:
Received xxxxx
Revised xxxxx
Accepted xxxxx
Available online xxxxx

Keywords:
Multi-fractal analysis,
Holder exponent,
Fractal dimension,
Emphysema identification,
HRCT images
Classification analysis.

ABSTRACT

Fractal dimension is a very useful metric for measuring the statistical self-similarity features of biomedical images. Its applications include shape classification, texture segmentation, and medical picture analysis. The most often used technique for determining the fractal dimension of digital images is the box-counting method. Using this crucial characteristic to categorize patterns in high resolution computed tomography images (HRCT) is also highly tough and demanding. In order to identify emphysema patterns in HRCT images, this study computed the Holder exponent of the local intensity values. A good statistical analysis of emphysema patterns depends on the absolute differences between the normal and pathological regions in the images. The outcomes of this study showed how well the features taken from the Holder exponent could predict outcomes when it comes to the interpretation and classification of HRCT scans. The overall classification accuracy in lung tissue layers is more than 90%, demonstrating the effectiveness of the techniques examined in this work.

1. Introduction

The majority of earlier research that made use of the emphysema database focused on classifying various emphysema pattern classes; nevertheless, another crucial issue that has to be looked into is the quantity and positions of the patterns inside an image [1-3]. The identification of the region of interest (ROI) using general or classical methodologies has been extensively studied [4,5]. In this scenario, the ROI in the images would be automatically identified by using the computation of the alpha values produced by the Holder exponent of the pixel intensity of the original HRCT image.

*Corresponding author: Musibau A. Ibrahim
E-mail address: kunle_ibrahim2001@yahoo.com
https://doi.org/10.60787/jnamp.v67i2.366

The prior work in [6–9] provided the computation of the Holder exponent of the original image of size M × N, which produces the corresponding alpha values that finally translate to alpha-images. When assessing the patterns and distribution of emphysema, high resolution computed tomography (HRCT) is a very useful scanning technique that is more sensitive than chest radiography. At this stage, HRCT is most helpful since some patients with early emphysema, especially those with early illness, may still have symptoms. Areas of abnormally low attenuation that are immediately distinguishable from the surrounding normal lung parenchyma are a symbol of emphysema on HHRCT [3,10]. Three classes can be used to categorize emphysema:

Centrilobular emphysema (CLE) is characterized by the presence of several small low-attenuation areas; paraseptal emphysema (PSE) is characterized by the presence of multiple low-attenuation areas in a single layer along the pleura, frequently encircled by interlobular septa that are discernible as thin white walls; and panlobular emphysema (PLE) is characterized by the presence of fewer and smaller pulmonary vessels in a low-attenuation lung. Figure 1 illustrates CLE and PSE examples along with normal tissue (NT) from HRCT images.

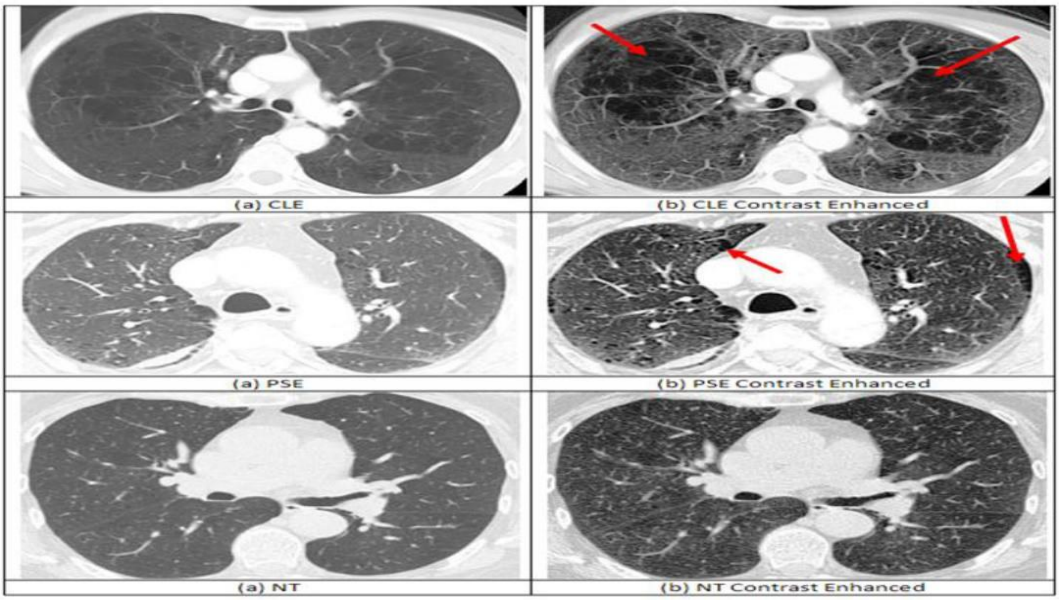

Figure 1: HRCT images showing emphysema disease patterns. The images in the first column were obtained from Radiopaedia [11].

Because the alpha value computation uses the pixel intensity distributions to disclose the local behavior or characteristics of the images, it may be a very useful tool for detecting and identifying an emphysema pattern in a specific place. By resolving the abnormalities found in biomedical images, it facilitates the process of identifying patterns. One highly potent and significant property of an alpha image is that it may be used to describe the image's local distinctive qualities in a unique way. It has an index to measure the local complexity of the tissue image, which is defined by variables such as the alpha values' lowest and maximum, the time interval between the two, and the variations in the mean alpha value with the standard deviation.

Moreover, the patches and the HRCT pictures might be used to derive the mentioned critical characteristic parameters for classification. In order to measure the mean alpha values of each class interval in terms of the frequency distributions of the alpha belonging to each class for additional analysis and investigations of the emphysema patterns, the average values of the class intervals of the alpha intensity values can also be calculated by dividing the alpha values.

ROI has already been located and identified in a variety of digital images using fractal dimension tools [14–17]. Different fractal dimension measurements can be used to vary the image complexities at different locations. For example, the CT images' emphysema containing regions or sections should be expected to be more complex than their non-emphysema counterparts, with higher fractal dimension values. Alzheimer's disease patients have also been diagnosed using fractal dimension. Gómez et al. [18] found that the Higuchi fractal dimension of the signals from Alzheimer's patients had lower FD values than those of the recorded control participants. The elderly control participants of Higuchi's dimension values do not differ statistically significantly from those of the Alzheimer disease patients. In order to increase computational accuracy and speed, Paramanathan et al. [19] computed the waveform's Higuchi's fractal dimension and set criteria for calculating the interval's minimum and maximum values.

In order to detect emphysema efficiently, this paper proposes the implementation of Holder exponent of the image intensity. As previously mentioned, the suggested system in this paper would be centered on identifying emphysema patterns using the fractal characteristics of the image textures. The absolute disparities in the overall mean values of the alpha values between the images of normal tissue and the images of histology might be used to accomplish the suggested concepts in a number of ways. While the regions without significant differences would undoubtedly not have any emphysema patterns, the regions with statistically significant absolute mean differences are more likely to possess emphysema patterns. The Higuchi's dimension analysis can be performed using the same process, with the result that the number of pattern detections would be reflected in the absolute variations in dimension between the normal and other classes.

A prior implementation and application of the Holder exponent of the local distribution of the intensity measure was made for the formation of the multi-fractal spectrum in CT images [5-8,20-21]. This paper would use the local descriptor (Holder exponent) of the CT images to detect the emphysema patterns, whereas the previous work applied a global descriptor (multi-fractal spectrum) for identifying different areas in biomedical images. This is the main distinction between the previous approaches and the proposed idea. The Holder exponent, which has been effectively applied as a global descriptor for effective classification in biomedical images, is the basis for the computation of a multi-fractal descriptor. However, since our goal is to identify patterns within the images, the Holder exponent may be more suitable for this purpose.

1. METHODS FOR DETECTING EMPHYSEMA PATTERNS

The general methods and statistical analysis used to find and recognize emphysema patterns in HRCT images by applying the Holder exponent methodology can be seen in Figure 2.

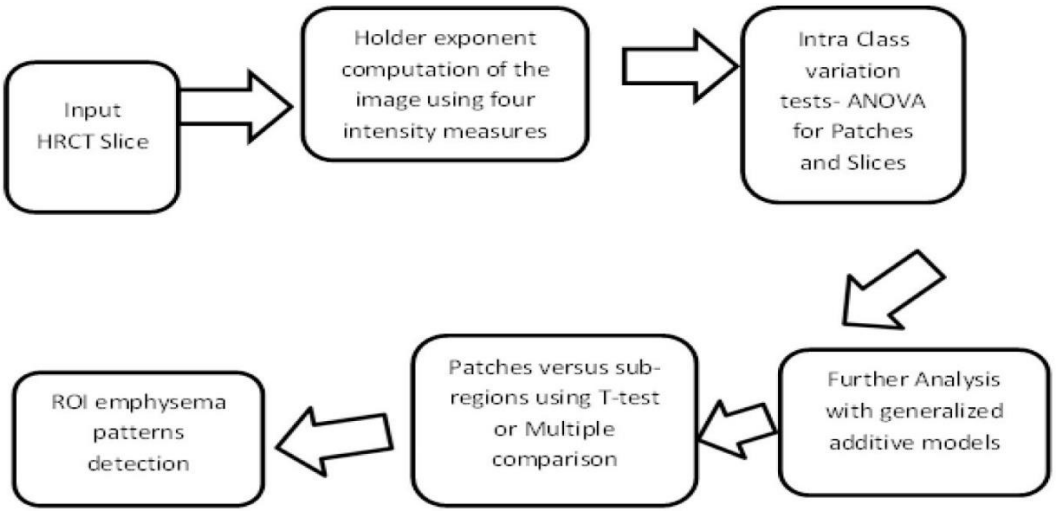

Figure 2: Holder exponent computation of emphysema pattern

Figure 2 provides a comprehensive summary of the steps involved in identifying emphysema patterns using absolute differences in alpha values. The computation of alpha values has been utilized in further analysis to detect patterns. For a classification process to be successful, there should be little intra-class variation in the images within the same group and a lot of inter-class diversity in the images between the groups. To ascertain how significant the differences between the images of various emphysema classes are, as well as how similar the images of the same emphysema classes inside the ground truth patches are, several preliminary statistical tests were therefore conducted.

The locations of the images with the emphysema patterns have been determined by additional statistical analysis; however, the methods employed to do this will be discussed later. The phrase "ground truth approach" refers to a method of drawing conclusions from data obtained through initial testing or observation. For every alpha image, an analysis of variance (ANOVA) has been computed using the local characteristic of the alpha intensity values. The differences between the ground truth images and the HRCT image slices have been measured using the alpha values of the HRCT images, which were calculated by using the Holder exponent. Additionally, absolute FDs differences were computed and employed for ROI detections across several locations between the histological images and normal tissues. The conclusions were derived from the statistical analysis, and the key elements of the slice images were utilized to confirm the algorithms' effectiveness. Developing an effective classification method for emphysema pattern detections has been made possible by the ground truth image findings, which indicated that the patches originated from the HRCT images. Three image slices were selected for comparison using alpha intensity values, and three patch images were chosen from each type of lung in this experiment. The ground truth images with labels were verified by comparing each segmented image in the slice with the ground truth patches.

2. RESULTS AND DISCUSSION

The techniques that were previously presented as shown in Figure 2 have been implemented to accurately detect emphysema patterns. Every image slice of 512 × 512pixel intensity has been split up into 64 smaller images. The 64 sub-images were arranged in an 8 × 8 matrix, with the numbers numbered from left to right and top to bottom. This meant that the first image corresponded to the matrix location in the first row and column, and the sub-image at the

matrix location in the eighth row and column corresponded to the sub-image number 64, and so on. The locations of the emphysema patterns were ascertained by comparing the absolute mean differences of the computed alpha-values produced by the Holder exponent approach between the images of normal tissues and that of emphysema, as well as the outcomes of the paired samples t-test. Table 1 displays the experiment results, including the group means and associated p-values for each experiment.

Table 1. Intra-Class variation between the patches and corresponding sub-image slices

Patches/Slices	Mean1	Mean2	*p*-values
NT1-NT1	1.9915	1.9949	.2947
CLE1-CLE1	1.9915	1.9961	.2907
PSE1-PSE1	1.9925	1.9965	.2919

Table 1 also showcase the mean alpha values for a subset of the divided images in each of the three emphysema classes. A selection of these images is provided to highlight the places with and without emphysema patterns. In order to identify the association between the classes, the mean alpha values in each class have been utilized to create the linear regression models using the smoothing techniques. It has been determined that the respective sub-images generated from the slices overlap each other, and that the group mean in each group falls between the emphysema class of the ground truth images. There are no visible changes between the images, according to the appropriate p-values for each test. According to Table 1's statistics, the estimated mean difference between the NT of the ground truth patches and the mean of the corresponding sub-image slice is -0.0033. This test indicates that the difference is not significant at the 0.05 level because the confidence interval contains 0.0.. That is, to identify the regions with the emphysema patterns in each sub-divided image, the absolute mean differences between normal tissues and CLE pair classes and the NT-CLE pair classes have been calculated. For example, based on the findings of the paired samples t-test, Table 1's absolute mean deviations between the normal tissues and the CLE and PSE classes showed that certain regions have emphysema patterns while others do not. The findings of the paired t-test demonstrated that, with a p-value <.001 and a 95% confidence interval on the mean that does not contain 0 exclusively in those regions with the emphysema patterns, the differences between the normal and emphysema images are statistically significant. In those areas lacking emphysema patterns, the p-values are higher than the significant level of .05.

These results are also in line with Figure 3, which were obtained using generalized regression models of the mean deviation values between the CLE classes and normal tissues. Figure 3 displays the findings of the absolute mean deviations of the normal tissues from different emphysema classes against sub-images. In this instance, despite a p-value <.0001 and a 95% confidence interval for the mean, sub-images in the 52–56 range exhibit larger deviation values than other locations. Since the paired sample t-test has confirmed that the differences are statistically significant, it suggests the existence of emphysema patterns in these specific regions. With very minor variations, these significant variances can be found in nearly the same places for both PSE and CLE. When checked, other variations throughout the graph's regions do not reveal statistically significant differences, suggesting that emphysema patterns are not present in these regions.

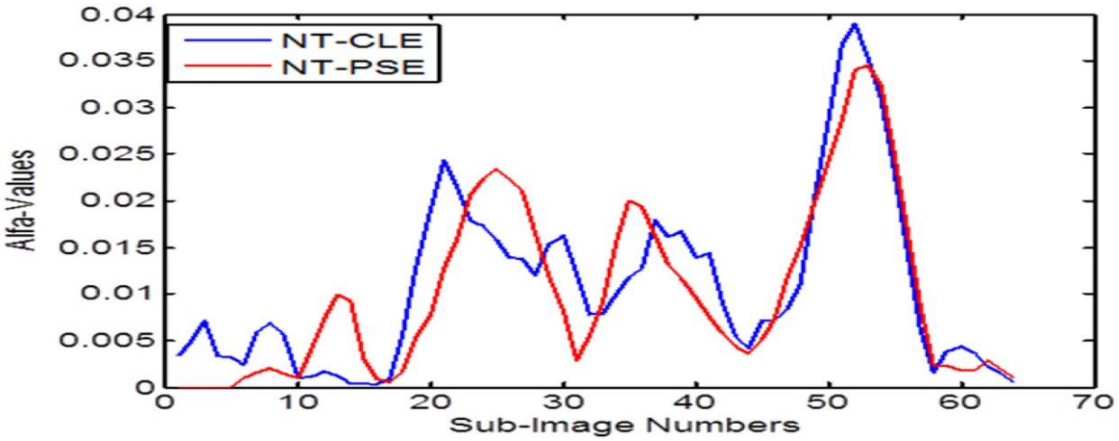

Figure 3: Mean deviations of normal tissues versus other classes in 64 × 64 sub-images

The HRCT image intensity distributions and the complexity of a given region are determined by the presence of emphysema patterns in those regions with higher mean deviations of the Holder exponent, or the alpha values. The mean deviations or variations between the normal and abnormal tissues are related to the irregularity of the imaging tissues. However, the presence of emphysema patterns increases with bigger absolute mean deviations from normal tissues and vice versa.

3. CONCLUSIONS

This paper has presented a few uses of Holder exponent in CT emphysema images. ROI in HRCT images can be identified and detected with high accuracy using the local intensity distributions, as demonstrated by the alpha values derived from the Holder exponent computation. Excellent performance has been achieved by using local characteristics of the image textures. The techniques proved to be a very excellent indicator and sufficiently precise to distinguish between areas with and without emphysema patterns. The developed system has proven to be useful and reliable, as evidenced by a classification accuracy of over 90% accuracy in lung tissue. Thus far, the results have demonstrated the potential effectiveness of both global features derived from the estimated Higuchi fractal dimension and local features extracted from the images for the analysis and categorization of the regions of interest. By using more accurate and efficient techniques to determine the fractal dimension of the CT scans or by verifying the computational accuracy and time complexity of the algorithms, further study in this field could be conducted. This study strategy can also be expanded by utilizing Higuchi's method within a multi-fractal framework. By doing so, it will be possible to compute the multi-fractal spectra of digital images, which can increase recognition accuracy.

REFERENCES

[1] Mendoza CS, Washko GR, Ross JC, et al. Emphysema Quantification in A Multi-Scanner HRCT Chort using Local Intensity Distributions. IEEE. 2022:474-7. PMid:23743800

[2]Nava R, Marcos JV, Escalante-ram B, et al. Advance in Texture Analysis for Emphysema Classification. Springer-Verlag Berlin Hei- delberg. 2023: 214-21. https://doi.org/10.1007/978-3-642 -41827-3_27

[3] Sorensen L, Shaker SB, De Bruijne M. Quantitative Analysis of Pulmonary Emphysema using Local Binary Patterns. IEEE Trans- actions on Medical Imaging. 2018; 29(2): 559-59. PMid:20129855 https://doi.org/10.1109/TMI.2009.2038575

[4] Irini R, Reljin B, Pavlovic I, et al. Mutifractal analysis of gray-scale images. Electrotechnical Conference. 2015; 2: 490-3.

[5] Polychronaki GE, Ktonas PY, Gatzonis S, et al. Comparison of fractal dimension estimation algorithms for epileptic seizure onset detection. Journal of Neural Engineering. 2021; 7(4): 046007. PMid:20571184 https://doi.org/10.1088/1741-2560/7/4/046007

[6] Hemsley A, Mukundan R. Multifractal Measures for Tissue Image Classification and Retrieval. IEEE International Symposium on Multimedia. 2019; 93(1): 618-23. https://doi.org/10.1109/ISM.2009.94

[7] Mukundan R, Ibrahim M. Multifractal Techniques for Emphysema Classification in Lung Tissue Images. International Conference on Future Bioengineering. 2014; 11 (2): 223-34.

[8] Ibrahim MA, Mukundan R. Cascaded techniques for improving emphysema classification in computed tomography images. Artificial Intelligence Research. 2015; 4(2): 112-8. https://doi.org/10.5 430/air.v4n2p112

[9] Hemsley A, Mukundan R. Tissue Image Classification Using Multi- Fractal Spectra. International Journal of Multimedia Data Engineering & Management. 2012; 1(2): 62-75.

[10] Chabat F, Yang GZ, Hansell DM. Obstructive lung diseases: texture classification for differentiation at CT. Radiology. 2023; 228(3): 871-7. PMid:12869685 https://doi.org/10.1148/radiol.2283020505

[11] Radiopaedia: A Wiki-based Collaborative Radiology Resource. Available from: http://radiopaedia.orgStern EJ, Swensen SJ, Kanne JP. High-Resolution CT of the Chest. Wolters Kluwer; 2020.

[12] Takahashi M, Fukuoka J, Nitta N, et al. Imaging of pulmonary emphysema: A pictorial review. International Journal of Chronic Obstructive Pulmonary Disease. 2022; 3(2): 193-204. PMid:18686729 https://doi.org/10.2147/COPD.S2639

[13] Soares F, Janela F, Pereira M, et al. Classification of Breast Masses on Contrast-Enhanced Magnetic Resonance Images Through Log Detrended Fluctuation Cumulant-Based Multifractal Analysis. IEEE Systems Journal. 2019; 8(3): 929-38. https://doi.org/10.110 9/JSYST.2013.2284101

[14] Iftekharuddin KM, Jia W, Marsh R, et al. A fractal analysis approach to identification of tumor in brain MR images. Machine Vision and Applicatons, Springer-Verlag. 2023; 13: 352-62. https://doi.org/10.1007/s00138-002-0087-9

[15] Liu JZ, Zhang LD, GH Yue. Fractal dimension in human cerebellum measured by magnetic resonance imaging. Biophysical Journal. 2019; 85(6): 4041-6.

https://doi.org/10.1016/S0006-3495(03)74817-6

[16] Kiselev VG, Hahn KR, Auer DP. Is the brain cortex a fractal? Neuroimage. 2023; 20(3): 1765-74. https://doi.org/10.1016/S1 053-8119(03)00380-X

[17] Gómez C, Mediavilla A, Hornero R. Use of the Higuchi's fractal dimension for the analysis of MEG recordings from Alzheimer's disease patients. Medical Engineering & Physics. 2009; 31(3): 306-13. PMid:18676171 https://doi.org/10.1016/j.medengphy.2008.06.010

[18] Paramanathan P. An algorithm for computing the fractal dimension of waveforms. Applied Mathematics & Computation. 2018; 195(2): 598-603. https://doi.org/10.1016/j.amc.2007.05.011

[19] Reljin IS, Reljin BD. Fractal geometry and multifractals in analyzing and processing medical data and images. Archive of Oncology. 2019; 10(4): 283-93. https://doi.org/10.2298/AOO0204283R

[20] Stojic´ T, Reljin I, Reljin B. Adaptation of multifractal analysis to seg- mentation of microcalcifications in digital mammograms. Physica A Statistical Mechanics & Its Applications. 2020; 367(June): 494-508.

Ibrahim MA. Multifractal techniques for analysis and classification of emphysema images. PhD thesis, University of Canterbury; 2017.ical education in science and technology,35:897-902